

Crystal growth and thermal conductivity of an Tm³⁺-doped Y₂O₃ for IR eye-safe laser

J. H. Mun^{a,*}, A. Jouini^b, A. Novoselov^c, A. Yoshikawa^c and T. Fukuda^c

^aGyeongbuk Hybrid Technology Institute, 36 Goeyeon-Dong, Yeongcheon, Gyeongbuk, 770-170, KOREA

^bPhysical Chemistry of Luminescent Materials, UMR 5620 CNRS, Claude Bernard/Lyon1 University, 69622 Villeurbanne, France

^cInstitute of Multidisciplinary Research for Advanced Materials, Tohoku University, 2-1-1 Katahira, Aoba-ku, Sendai 980-8577, Japan

Refractory undoped and Tm³⁺-doped (0.15, 1, 3 and 5 mol.%) Y₂O₃ single crystals were grown by the micro-pulling-down method. Chemical analysis showed a homogeneous distribution of Tm³⁺ dopant along the crystal rod. The dependence of thermal conductivity on Tm³⁺ concentration in Tm³⁺:Y₂O₃ was characterized. The value decreases when the Tm³⁺ concentration increases in the host but still stays high enough (7.46 Wm⁻¹K⁻¹) when doped with Tm³⁺ (5 mol.%), which represents a promising material for an infrared eye-safe laser application.

Key words: Tm³⁺ activator, Thermal conductivity, Micro-pulling-down method, Crystal growth from the melt, Rare-earth sesquioxides, Solid-state laser host.

Introduction

In recent years laser action in trivalent Tm³⁺, Ho³⁺ and Er³⁺ have gained a large interest and a rapid development. The main interest in the 2 μm laser on the ³H₄ → ³H₆ transition arises from its applications in medicine and remote sensing. Despite its success, however, some key problems still remain unsolved. These include a severe dependence on pump diode temperature control due to the relatively narrow Tm³⁺ absorption lines in hosts like Y₃A₁₅O₁₂ (YAG) and YLiF₄ (YLF). In the case of longitudinal pumping, a further drawback of YAG and YLF is the requirement of low numerical aperture pump beams for efficient overlap of pump and resonator modes over relatively long crystals. Crystal length is dictated by the low absorption in these materials. In addition, Tm³⁺ absorption peaks are shifted to a shorter wavelength with respect to neodymium, for which the bulk of commercially available laser diodes (LD) are prepared [1].

Besides, Tm³⁺-doped materials can be used for such eye-safe laser applications as lidar-sensing [2] and medical scalpels [3, 4]. Since water, namely tears in eyes, absorbs radiation having wavelength above 1.4 μm, wavelengths around 1.5-2 μm are suitable for the eye-safe laser and accordingly Tm³⁺, Ho³⁺ and Er³⁺ are candidates as active ions for solid-state laser sources. Among these ions, Tm³⁺ is suitable for LD pumping, which is already usually used for the Nd³⁺ lasers, since Tm³⁺ has an appreciably wide

absorption band around 800 nm nearby Nd³⁺ absorption one. A variety of solid-state lasers have been constructed for eye-safe applications using Tm-doped YAG [5, 6], YLF [7, 8] and REVO₄ (RE: Y and Gd) [9-11]. The broad emission spectrum (1.9-2.1 μm) allows tuning the laser wavelength and generation of ultra-short pulses [12].

Refractory rare-earth sesquioxides (RE₂O₃, RE = Y, Lu and Sc) seem to be promising host materials for solid-state lasers due to their high thermal conductivity and low phonon energy. For example, the large thermal conductivity of refractory Y₂O₃ (13.6 W m⁻¹ K⁻¹ at 300 K) is very favorable for efficient cooling of the crystal [13]. The thermal conductivity of Y₂O₃ is more than a factor of two higher than that of YVO₄ and is even higher than that of YAG. These properties favor this material as a host crystal for high-power solid-state lasers. The effective phonon energies of Y₂O₃ and Lu₂O₃ are quite low compared to other oxides. Weber [14] reported a value of only 430 cm⁻¹ which is much lower than, for example, 700 cm⁻¹ for YAG. A low phonon energy means low non-radiative transition rates of metastable electronic levels and therefore high quantum efficiency.

However, the high-melting point of Y₂O₃, Sc₂O₃ and Lu₂O₃ of above 2400 °C hinders the growth of single crystals from crucibles. Growth methods that were established for the growth of the high-melting sesquioxides are the Verneuil method, the flux method and the laser heated pedestal growth technique [15]. These methods are limited as far as the size and optical quality of the crystals

In this paper, we will report the optimization of the growth conditions for bulk single crystal growth of Tm³⁺:Y₂O₃ by the micro-pulling-down (μ-PD) method which was successfully used to grow Yb³⁺-doped Y₂O₃ [16]. In addition,

*Corresponding author:
Tel : +82-54-330-8012
Fax: +82-54-330-8019
E-mail: jhmun@ghi.re.kr

thermal conductivity of $\text{Tm}^{3+}:\text{Y}_2\text{O}_3$ was characterized using the results of thermal diffusivity and heat capacity measurements and the corresponding results will be listed.

Experimental

The high melting point of yttria (2410 °C) restricts the choice of crucible materials. The crucible has to be mechanically stable at the melting point of the growing oxide and must be resistant against chemical reactions with the melt as well as with the surrounding thermal insulation. Rhenium fulfills these requirements to the greatest extent.

Single crystal growth was performed by the μ -PD method using a rhenium crucible 46 mm in height and 36 mm in diameter. The starting materials were prepared from high-purity commercial powders of Y_2O_3 (> 99.99%) and Tm_2O_3 (99.99%). The starting melt composition of $(\text{Tm}_x\text{Y}_{1-x})_2\text{O}_3$ was varied as $x = 0.0, 0.0015, 0.01, 0.03$ and 0.05 . The crucible was completely surrounded by insulation material such as zirconia and quartz tubes and heated using a radio-frequency generator. The raw materials were melted in the rhenium crucible and allowed to pass through the micro-nozzle. The single crystal was formed by attaching the seed to the crucible tip and slowly pulling downward with a constant velocity. A Y_2O_3 single crystal rod was used as a seed. The growth atmosphere was mixture of Ar + H_2 (3 vol%). After growth, the crystals were cooled down to room temperature at a rate of 1073 K h^{-1} .

In order to identify the phase obtained, powder X-ray diffraction analysis was carried out using a RINT-2000 (RIGAKU) diffractometer with $\text{CuK}\alpha$ X-rays. The diffraction pattern was scanned over the 2θ range 10 – 80° with steps of 0.02° . The accelerating voltage was 40 kV and the current was 40 mA. All the X-ray experiments were carried out at room temperature.

The chemical composition was analyzed by electron probe microanalysis (EPMA) using JEOL JXA-8621MX. The distribution of cations in the single crystal was measured along the growth axis using an electron probe a $10 \mu\text{m}$ in diameter.

The crystallinity was investigated by X-ray rocking curve (XRC) analysis for the (2 2 2) plane of the grown Y_2O_3 crystals using a high-resolution diffractometer (RIGAKU ATX-E) with $\text{CuK}\alpha_1$ radiation diffracted by a four-crystal Ge (2 2 0) channel monochromator. Crystallinity of the grown Y_2O_3 crystal was evaluated based on the full-width at half-maximum (FWHM) of the (2 2 2) peak.

Thermal diffusivity was measured under vacuum by a laser flash method [17]. Each crystal was cut into a disk shape with a size of 0.5 mm in thickness and 4.2 mm in diameter and the surface was coated with gold by a sputtering process in order to avoid the penetration of the laser light. Specific heat capacity was measured with a differential scanning calorimeter (DSC) apparatus in the temperature range from 523 K to 823 K. The measurement was carried out in a high purity argon atmosphere with a flow rate a $20 \text{ ml minute}^{-1}$ to prevention of oxidation.

A Au cell with in 5 mm diameter, 2.5 mm height and 0.2 mm thickness was used as a cell from 523 K to 823 K. The weight of the samples was about 30 mg. The specific heat capacity of $\alpha\text{-Al}_2\text{O}_3$ was used as a reference.

Results and Discussion

The transparent, crack and inclusion-free $\text{Tm}^{3+}:\text{Y}_2\text{O}_3$ single crystals were grown by the μ -PD method for each Tm concentration (0, 0.15, 1, 3 and 5 mol.%).

Fig. 1 shows the as-grown $\text{Tm}^{3+}:\text{Y}_2\text{O}_3$ single crystals. The crystal dimensions were about 4.2 mm in diameter and 10–20 mm long. The growth was performed under an Ar + 3 vol% H_2 atmosphere and a pulling rate of 0.05 to $0.2 \text{ mm minute}^{-1}$. These crystals were colored very weakly in gray and blue and the color became slightly stronger with an increase in the Tm concentration. As-grown crystals were annealed at $1450 \text{ }^\circ\text{C}$ for 30 h in air to remove the coloration (Fig. 1).

Evolution of the powder X-ray diffraction pattern as a function of the Tm concentration was investigated. A single phase was formed in all the concentration range and no impurity phase was detected. The lattice constant became systematically smaller with the Tm concentration as shown in Fig. 2. This result is in good agreement with Vegard's law.

The Tm^{3+} distribution was investigated using EPMA.

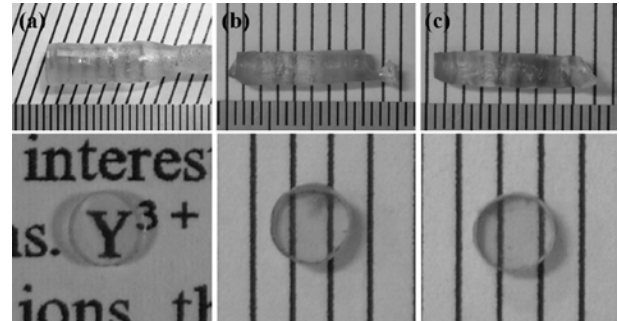


Fig. 1. Photographs of as-grown $(\text{Tm}_x\text{Y}_{1-x})_2\text{O}_3$ single crystals and samples cross-sections after annealing in air at $1450 \text{ }^\circ\text{C}$ for 30 h. (a) $x = 0.0$, (b) $x = 0.0015$, (c) $x = 0.01$.

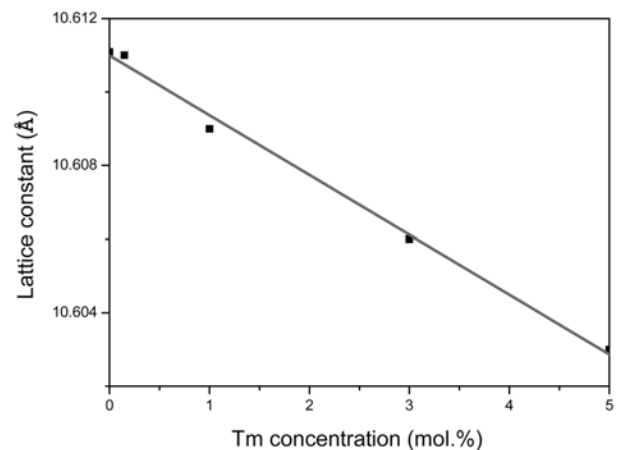


Fig. 2. Concentration dependency of lattice constants of $(\text{Tm}_x\text{Y}_{1-x})_2\text{O}_3$.

Fig. 3 illustrates that $Tm^{3+} : Y_2O_3$ crystals grown by the μ -PD method have a good compositional homogeneity along the growth axis. Tm^{3+} was homogeneously distributed in the Y_2O_3 host from the top to the end and the effective segregation coefficient of each constituent of the $Tm^{3+} : Y_2O_3$ melt became unity along the growth axis leading to a homogeneous composition throughout the crystal.

Fig. 4 shows a typical XRC of undoped Y_2O_3 and 5% Tm-doped crystals. In this experiment, the (2 2 2) reflection of $CuK\alpha_1$ X-rays was employed to study the evolution of crystallinity. The diffraction curve is quite sharp with a FWHM value of ~ 68.4 arcs. In the case of the 5% Tm-doped crystal, the FWHM value was ~ 82.8 arcs. According to the results of these measurements, the samples studied have as good crystallinity as that of other optical grade crystals.

Thermal diffusivity of undoped and Tm-doped Y_2O_3 was measured at room temperature under a vacuum of less than 10 Pa by a laser flash method. A Nd:glass laser instantaneously irradiated the upper surface of a specimen. Then, the temperature response at the bottom surface of the specimen was measured using an InSb infrared detector.

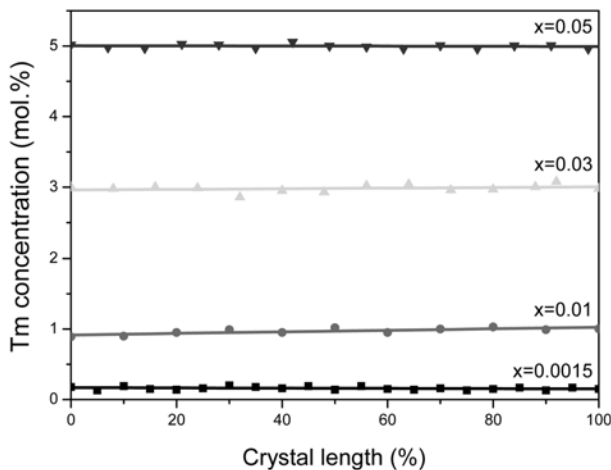


Fig. 3. Tm^{3+} distribution along the growth axis for $(Tm_x Y_{1-x})_2O_3$, $x = 0.0015, 0.01, 0.03$ and 0.05 crystals.

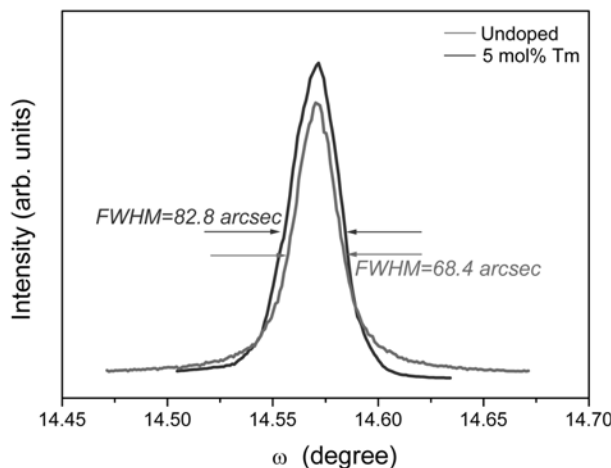


Fig. 4. X-ray rocking curve of undoped and Tm (5 mol.%) Y_2O_3 doped single crystals. The peak from the (2 2 2) plane was employed.

Fig. 5 shows the measured temperature response curve of undoped- Y_2O_3 and the thermal diffusivity was determined using the following equation:

$$\alpha = \frac{1.37 \cdot L^2}{\pi^2 \cdot t_{1/2}} \quad (1)$$

where L is sample thickness and $t_{1/2}$ is the time to reach a half of a maximum temperature rise. The thermal diffusivity of Tm-doped Y_2O_3 decreases with the Tm^{3+} dopant content increase and the measured values are summarized in Table 1. The specific heat capacity is one of the important factors that influence the damage threshold of a crystal. Here, we could measure the area of the sapphire, the sample and the holder by using the Origin program, and calculate the specific heat capacity of undoped and Tm^{3+} -doped Y_2O_3 using the following equation:

$$C_{pS} = \frac{C_{pR} \cdot W_R \cdot S_S}{W_S \cdot S_R}, \quad (2)$$

where C_{pS} is specific heat capacity of the sample, W_S - the sample weight, C_{pR} - the specific heat capacity of sapphire, W_R - the sapphire weight, S_S - DSC signal real area of the sample ($H_S - H_{ES}$), S_R - DSC signal area of the sapphire ($H_R - H_{ES}$)

In the case of undoped- Y_2O_3 , the heat capacity was

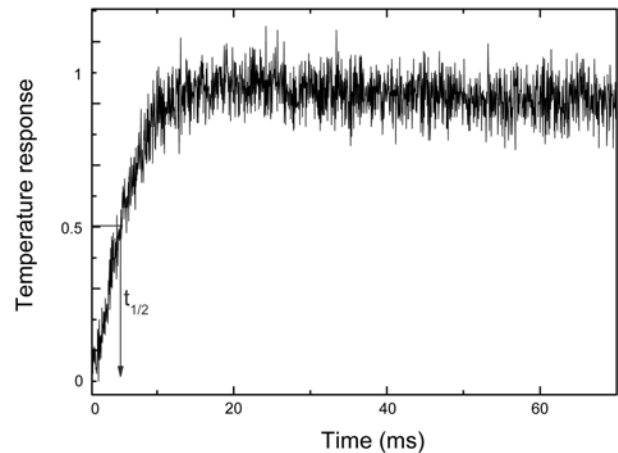


Fig. 5. Temperature response curve of undoped Y_2O_3 in a thermal diffusivity measurement.

Table 1. Thermal diffusivity, density, heat capacity and calculated thermal conductivity of the undoped and Tm-doped Y_2O_3 crystals studied

Tm content (mol%)	Thermal diffusivity ($\times 10^{-6} m^2/s$)	Density (g/cm^3)	Specific heat capacity ($Jg^{-1}K^{-1}$)	Thermal conductivity ($Wm^{-1}K^{-1}$)
0	7.20	5.030	0.440	15.94
0.15	7.20	5.044	0.430	15.61
1	5.93	5.075	0.420	12.64
3	3.80	5.146	0.418	8.17
5	3.55	5.218	0.403	7.46

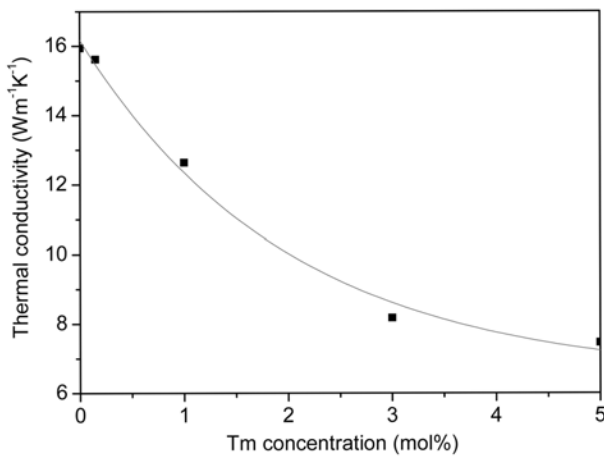


Fig. 6. Tm concentration dependence of the thermal conductivity in Tm : Y₂O₃.

0.44 Jg⁻¹K⁻¹ at room temperature. The numerical data for Yb-doped samples are also presented in Table 1. The specific heat capacity of Y₂O₃ increase linearly with an increase of the temperature in the range from 523 K to 823 K. As the Tm³⁺ dopant content increases, the heat capacity increases.

Thermal conductivity was calculated from thermal diffusivity (α), heat capacity (C_p), and density (ρ) (undoped Y₂O₃, $\rho = 5.03$ g/cm³ [18]) using the following expression:

$$\lambda = \alpha \cdot C_p \cdot \rho \quad (3)$$

Fig. 6 shows the thermal conductivity versus the Tm³⁺ dopant content in Y₂O₃.

The value of thermal conductivity of Tm³⁺-doped Y₂O₃ decreases with an increase of the Tm³⁺ content. The value of the thermal conductivity of undoped-Y₂O₃ is 15.94 Wm⁻¹K⁻¹ at room temperature and 7.46 Wm⁻¹K⁻¹ when doped with Tm (5 mol.%).

Conclusions

Refractory Tm³⁺-doped Y₂O₃ single crystals were successfully grown by the μ -PD method using a rhenium crucible. The best single crystals were obtained with a pulling-down rate equal to 0.1 mm minute⁻¹. Tm³⁺-doped Y₂O₃ single crystals had a good compositional homogeneity in the pulling-down axis and the lattice constant became systematically smaller with an increase of the Tm³⁺ concentration.

The thermal properties which are very important parameters for laser crystals have been measured: thermal

diffusivity of undoped-Y₂O₃ was characterized as 7.20 $\times 10^6$ m² s⁻¹, heat capacity has been measured from 523 K to 823 K and the thermal conductivity of both undoped Y₂O₃ and Tm³⁺-doped Y₂O₃ was obtained using these data. The value of the thermal conductivity of undoped Y₂O₃ is as high as 15.94 Wm⁻¹K⁻¹ at room temperature. The value decreases when the Tm³⁺ concentration increases in the host but still stays high enough (7.46 Wm⁻¹K⁻¹) when doped with Tm³⁺ (5 mol.%), which represents a promising material for infrared eye-safe laser application

References

1. C.P. Wyss, W. Lüthy, H.P. Weber, V.I. Vlasov, Y.D. Zavartsev, P.A. Studenikin, A.I. Zagumennyi and I.A. Shcherbakov, *Opt. Commun.* 153 (2001) 63.
2. S.W. Henderson, P.J.M. Suni, C.P. Hale, S.M. Hannon, J.R. Magee, D.L. Bruns and E.H. Yuen, *IEEE Trans. Geosci. Remote Sens.* 31 (1993) 4.
3. T. Becker, G. Hiber, H.J.V.D. Heide, P. Mitzscherlich and B. Struve, E.W. Duczynski, *Opt. Commun.* 80 (1990) 47.
4. R.C. Stoneman and L. Esterowitz, *Opt. Photonics News* 1 (1990) 10.
5. A. Rameix, C. Borel, B. Chambaz, B. Ferrand, D.P. Shepherd, T.J. Warburton, D.C. Hanna and A.C. Tropper, *Opt. Commun.* 142 (1997) 239.
6. C. Bollig, W.A. Clarkson, R.A. Hayward and D.C. Hanna, *Opt. Commun.* 154 (1998) 35.
7. I. Razumova, A. Tkachuk, A. Nikitichev and D. Mironov, *J. Alloy. Compd.* 225 (1995) 129.
8. T. Yokozawa, J. Izawa and H. Hara, *Opt. Commun.* 145 (1998) 98.
9. G. Lescroart, R. Muller and G. Bourdet, *Opt. Commun.* 143 (1997) 147.
10. C.P. Wyss, W. Lüthy, H.P. Weber, V.I. Vlasov, Y.D. Zavartsev, P.A. Studenikin, A.I. Zagumennyi and I.A. Shcherbakov, *Opt. Commun.* 153 (1998) 63.
11. Y. Urata, K. Akagawa, S. Wada, H. Tashiro, S.J. Suh, D.H. Yoon and T. Fukuda, *Cryst. Res. Technol.* 34 (1999) 141.
12. P.J. Morris, W. Lüthy, H.P. Weber, Yu.D. Zavartsev, P.A. Studenikin, I. Shcherbakov and A.I. Zagumennyi, *Opt. Commun.* 111 (1994) 493.
13. K. Petermann, G. Huber, L. Fornasiero, S. Kuch, E. Mix, V. Peters, S. A. Basun, *J. Lumin.* 973 (2000) 87.
14. M.J. Weber, *Phys. Rev.* 171 (1968) 283.
15. L. Laversenne, C. Goutaudier, Y. Guyot, M. -Th. Cohen-Adad and G. Boulon, *J. Alloy. Compd.* 341 (2002) 214.
16. J.H. Mun, A. Novoselov, A. Yoshikawa, G. Boulon and T. Fukuda *Mater. Res. Bull.* 40 (2005) 1235.
17. H. Shibata, H. Ohta, A. Suzuki and Y. Waseda, *Mater. Trans. JIM* 41 (2000) 1616.
18. F. Hanic, M. Hartmanova, G. G. Knab, A. A. Urusovskaya and K. S. Bagdasarov, *Acta Cryst.* B40 (1984) 76.